

Theory of Electrically Detected Magnetic Resonance of Silicon Vacancy-Related Spin Pairs in Silicon Carbide

David A. Fehr,¹ Corey J. Cochrane,² Stephen R. McMillan,³ Nicholas J. Harmon,⁴ Patrick M. Lenahan,⁵ and Michael E. Flatté¹

¹*Department of Physics and Astronomy, University of Iowa, Iowa City, Iowa 52242, USA*

²*Jet Propulsion Laboratory, California Institute of Technology, Pasadena, California 91011, USA*

³*Donostia International Physics Center, Donostia-San Sebastián, Spain*

⁴*Department of Physics and Engineering Science, Coastal Carolina University, Conway, South Carolina 29528, USA*

⁵*Department of Engineering Science and Mechanics, The Pennsylvania State University, University Park, Pennsylvania 16802, USA*

(*Electronic mail: david-fehr@uiowa.edu)

(Dated: 26 May 2026)

We present a quantitative theory for simulating the electrically detected magnetic resonance (EDMR) of silicon vacancy-related spin pairs in silicon carbide using steady-state Lindblad master equations. In our theory, we consider V1a and V2a deep level silicon vacancies near the (0/-) charge state transition level in proximity to a previously identified nitrogen-related complex, the incomplete K-center, due to the hyperfine, spin structure, and Landé g factor of the shallow state. Our theory describes recent room temperature measurements attributed to V1a silicon vacancies, with reasonable extracted parameters for defect spin coherence times and electrical transport rates. At lower temperatures we predict that the shallow level hyperfine structure may be spectrally resolvable. Finally, we predict the EDMR spectrum of V2a silicon vacancy-related spin pairs and predict that two-photon, double quantum transitions of the silicon vacancy's negative charge state can be electrically read-out for enhanced magnetic field sensing.

Silicon carbide (SiC) has emerged as an important material for power electronics beyond silicon due to its wide bandgap, enabling devices with higher operating temperatures and breakdown voltages, faster switching, and superior radiation hardness¹. SiC is also known to host electrically-active deep-level defects, both natively and resulting from irradiation, which limit device performance^{2,3}, and, in extreme cases, cause device failure⁴. On the other hand, some of these deep-level defects, namely silicon vacancies, have desirable quantum properties such as long coherence times⁵, optical^{6,7} and electrical^{8–11} readout modalities, and have great potential as quantum sensors of magnetic fields^{6,8–10,12,13} and temperature^{12,14}. Although defect-based quantum sensing schemes typically utilize optical readout for enhanced sensitivity, devices employing electrical readout such as electrically detected magnetic resonance (EDMR) do not require optics, making them easier to integrate with electronic circuitry and benefit from reduced size, weight, and power (SWaP).

In EDMR, an applied bias generates a non-equilibrium population of electrons and holes in the active region of the device. In subsequent electron-hole recombination which produces a spin-dependent recombination (SDR) current, a carrier is first captured by a shallow level defect and then by a deep level defect. Depending on the resulting angular momentum selection rules a Pauli-spin blockade occurs, bottlenecking the SDR current, which is relieved when one of the paired spins is resonantly flipping. This is accomplished with the application of a quasi-static magnetic field, which brings the energy levels of one or both spins into resonance with an applied oscillating magnetic field, relieving the bottleneck and producing a characteristic change in the measured SDR cur-

rent. A detailed and fully-quantitative theory of the recombination mechanism of silicon vacancy-related spin pairs is crucial to optimizing SiC power electronics and EDMR-based magnetometer technology.

Here we present a quantitative theory for simulating EDMR measurements of silicon vacancy-related spin pairs in 4H-SiC and compare with experimental results from Ref. 8. We first show results for V1a-type silicon vacancies (zero-field splitting $\mathcal{D} \simeq 0$ MHz), then V2a-type ($\mathcal{D} \simeq 35$ MHz)^{15,16}, and end with a full mathematical description of the model. In our model, the silicon vacancy is near the $q_V = (0/-)$ charge state transition level¹⁷, corresponding to the spin quantum numbers $S_V^{[q]} = (1/\frac{3}{2})$. To make a charge transition from the neutral to negative state, it must accept an electron from a "nearby" (within ~ 10 nm)^{18,19} shallow *donor* in the $q_S = (0/+)$ level, corresponding to the spin quantum numbers $S_S^{[q]} = (\frac{1}{2}/0)$. Thus, this transition is only allowed when the vacancy and donor electron spins are aligned **parallel**, as shown in Fig. 1. On the other hand, the silicon vacancy could make a charge transition from the negative to neutral state by accepting a hole from a "nearby" shallow *acceptor* in the $q_S = (0/-)$ level, again corresponding to $S_S^{[q]} = (\frac{1}{2}/0)$. Thus, this transition is only allowed when the vacancy and acceptor hole spins are aligned **antiparallel**, as shown in Fig. S1 in the Supplementary Information. The Hamiltonians of the shallow level spin center and the deep level silicon vacancy have the form:

$$\hat{H}_S = g_S \mu_B \left(\vec{B}_0 + \vec{B}_1(t) \right) \cdot \vec{S}_S + A_{S\parallel} \hat{S}_{S,z} \otimes \hat{I}_{S,z} \quad (1)$$

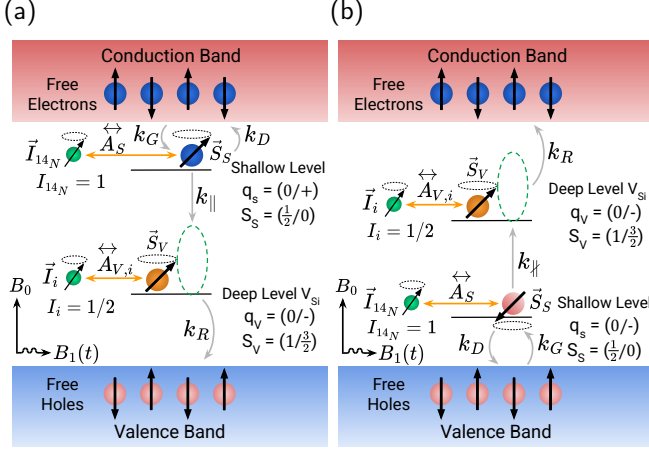


FIG. 1. EDMR diagram of silicon vacancy-related spin pairs in 4H-SiC. The silicon vacancy is in the $(0/-)$ charge and $(1/3/2)$ spin state level, and interacts with a dilute bath of proximal ^{29}Si and ^{13}C nuclear spins of nuclear spin magnetic moment $I_i = 1/2$. The shallow level spin center is $S = 1/2$ when neutrally charged and $S = 0$ when ionized, and interacts with a single onsite ^{14}N nuclear spin. (a) Shallow donor model. Non-spin-polarized conduction electrons are captured by the shallow donor, generating the spin pair at a rate k_G . From there, the unpaired electron can tunnel to the neutrally-charged silicon vacancy at a rate k_{\parallel} when the two spins are in a parallel configuration. Otherwise, the spin pair dissociates by depopulating the shallow level at a rate k_D . After the silicon vacancy becomes negatively-charged, it may release one electron to recombine with an anti-parallel-aligned valence hole at a rate k_R . (b) Shallow acceptor model. Non-spin-polarized valence holes are captured by the shallow donor, generating the spin pair at a rate k_G . From there, the unpaired hole can tunnel to the negatively-charged silicon vacancy at a rate k_{\parallel} when the two spins are in an anti-parallel configuration. Otherwise, the spin pair dissociates by depopulating the shallow level at a rate k_D . After the silicon vacancy becomes neutrally-charged, it may release one hole to recombine with a parallel-aligned conduction electron at a rate k_R .

$$\hat{H}_V^{[q]} = \mathcal{D}^{[q]} \left(\left[\hat{S}_{V,z}^{[q]} \right]^2 - \frac{1}{3} S_V^{[q]} (S_V^{[q]} + 1) \hat{I} \right) + \hat{S}_{V,z}^{[q]} \otimes \sum A_{V\parallel,i}^{[q]} \hat{I}_{i,z} + g_V^{[q]} \mu_B \left(\vec{B}_0 + \vec{B}_1(t) \right) \cdot \vec{S}_V^{[q]} \quad (2)$$

where \hat{H}_V and \hat{H}_S are the respective Hamiltonians of the silicon vacancy and the (occupied) shallow level spin center, $[q]$ denotes the charge state of the silicon vacancy, \vec{S} is the vector of spin operators, \mathcal{D} is the zero-field splitting, μ_B is the Bohr magneton, \vec{B}_0 is the applied magnetic field taken to be along $\hat{e}_z \parallel \hat{c}$, $|\vec{B}_1(t)| = B_1 \cos(\omega t)$ is the microwave field taken to be along \hat{e}_x with frequency ω , g_V and g_S are the g-factors of the vacancy and shallow level spins, $A_{\parallel,k}$ are the hyperfine tensor components parallel to \vec{B}_0 , and \hat{I}_k are nuclear spin operators.

We simulate the EDMR spectrum of silicon vacancy-related spin pairs in 4H-SiC with a three-manifold model. For the shallow donor (acceptor) case, the first manifold tracks the dynamics of the neutral (negative) charged silicon vacancy while the shallow level is *unoccupied*. The second manifold tracks the dynamics of the neutral (negative) charged silicon vacancy

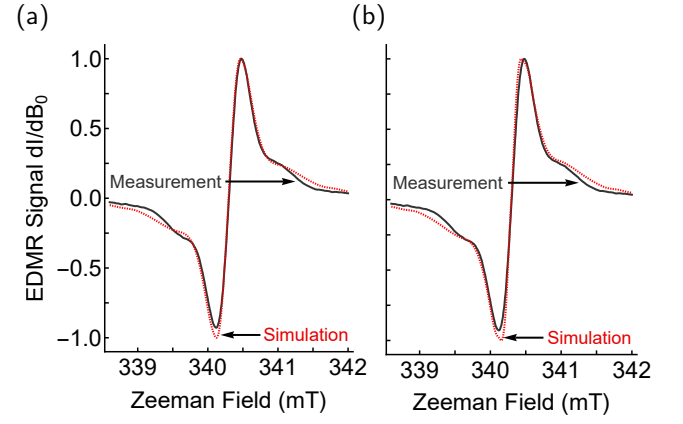


FIG. 2. EDMR spectrum (dI/dB_0) of V1a silicon vacancy-related spin pairs in 4H-SiC normalized to the peak height versus magnetic field with a microwave frequency of 9.54 GHz. The simulated spectra (dashed red) is compared to the room-temperature measurement (solid black) in Ref. 8. (a) Shallow donor model. (b) Shallow acceptor model, donor parameters $\times 3/4$ and $k_{\parallel} \rightarrow k_{\parallel}$. (Insets): Corresponding simulation and measurement⁸ of the integrated EDMR spectrum $I(B_0)$ versus magnetic field.

while the shallow level is *occupied*. The third manifold tracks the dynamics of the negative (neutral) charged silicon vacancy while the shallow level is again unoccupied. We ignore any coherence that may evolve at the shallow level when the deep level is negative (neutral) charged. We define the Hamiltonians for each of these configurations in terms of $\hat{H}_V^{[q]}$ and \hat{H}_S for the shallow donor case as $\hat{H}_{1\otimes 0} \equiv \hat{H}_V^{[0]}$, $\hat{H}_{1\otimes 1/2} \equiv \hat{H}_V^{[0]} \otimes \hat{I}_{1/2} + \hat{I}_1 \otimes \hat{H}_S$, and $\hat{H}_{3/2\otimes 0} \equiv \hat{H}_V^{[-]}$, respectively, where the subscripts label the respective spins of the deep and shallow levels and the superscripts label the spinful charge states. Thus, the total Hamiltonian $\mathcal{H}(t)$ is block diagonal in $\hat{H}_{1\otimes 0}$, $\hat{H}_{1\otimes 1/2}$, and $\hat{H}_{3/2\otimes 0}$. Similarly, for the shallow acceptor case we have $\hat{H}_{3/2\otimes 0} \equiv \hat{H}_V^{[-]}$, $\hat{H}_{3/2\otimes 1/2} \equiv \hat{H}_V^{[-]} \otimes \hat{I}_{1/2} + \hat{I}_{3/2} \otimes \hat{H}_S$, and $\hat{H}_{1\otimes 0} \equiv \hat{H}_V^{[0]}$, and the total Hamiltonian $\mathcal{H}(t)$ is block diagonal in $\hat{H}_{3/2\otimes 0}$, $\hat{H}_{3/2\otimes 1/2}$, and $\hat{H}_{1\otimes 0}$. In either case, our simulations are most sensitive to the dynamics of $\hat{H}_{1\otimes 1/2}$ (donor model) and $\hat{H}_{3/2\otimes 1/2}$ (acceptor model). To simulate the bath of ^{29}Si and ^{13}C nuclear spins ($I = 1/2$ in 4.7% and 1.1% abundance, respectively) in the vicinity of the silicon vacancy, we calculate EDMR spectra of the most likely configurations and perform a weighted sum by their respective probabilities of occurrence. All combinatoric details can be found in the Supplementary Information.

EDMR simulations from our theory of V1a silicon vacancy-related spin pairs in 4H-SiC are shown in Figures 2 and 3 as functions of the applied Zeeman magnetic field and at a constant microwave frequency of $f = \omega/2\pi \simeq 9.54$ GHz. Figure 2 shows the best-fit simulations to a room temperature EDMR measurement⁸, attributed to V1a silicon vacancy-related spin pairs in 4H-SiC. We use the same spin Hamiltonian parameters for both charge states of the V1a silicon vacancy as, to our knowledge, the literature lacks di-

rect measurements of these quantities for the neutral charge state, namely^{16,20,21}: $\mathcal{D}^{[0]} = \mathcal{D}^{[-]} = 0$, $g_V^{[0]} = g_V^{[-]} = 2.003$, $A_{\parallel,29Si}^{[0]} = A_{\parallel,29Si}^{[-]} = 8.35$ MHz, $A_{\parallel,13Cb}^{[0]} = A_{\parallel,13Cb}^{[-]} = 35$ MHz, and $A_{\parallel,13Ca}^{[0]} = A_{\parallel,13Ca}^{[-]} = 80$ MHz. Importantly, we found that the hyperfine splitting of the silicon vacancy was not sufficient to produce the subtle shoulders in the measurement. Thus, we conclude that these features must arise from hyperfine splitting of the shallow level spin's spectrum, which must have a g-factor near 2.003 and a hyperfine coupling of $\simeq 30.8$ MHz (if $I = 1/2$) or $\simeq 15.4$ MHz (if $I = 1$) according to the analysis in Ref. 8. Importantly, these constraints on the shallow level spin Hamiltonian parameters preclude the simple substitutional centers^{22–26}: nitrogen, phosphorus, boron, and aluminum.

Previously, this spin pair has been linked to a ^{14}N nuclear spin ($I = 1$) in EDENDOR measurements²⁷, and a recent EDMR measurement extracted the g-factor ($\simeq 2.003$) and hyperfine coupling (0.57 mT $\simeq 16$ MHz) between this nuclear spin and an unpaired electron spin²⁸. This EDMR spectrum was tentatively attributed to an “incomplete K-center” structure - a silicon dangling bond center with a single ^{14}N substituting onto one of the basal carbon sites, whose charge nature (i.e. donor or acceptor) is unknown. In our theory, we ascribe the shoulders in the measurement to this same structure, as the hyperfine coupling and g-factor match the requirements exactly. ^{14}N can occur in 4H-SiC defect complexes as it is commonly used as an n -type dopant and can be introduced through nitric oxide anneals^{29–32}, the latter being the case for the sample measured in Ref.8. Thus, for the shallow level spin Hamiltonian parameters we used $g_S = 2.003$ and $A_{\parallel,14N} = 0.57$ mT = 16.0 MHz.

In our best fits in Figure 2 we left the coherence times of both spins, microwave field strength B_1 , and the hopping rates as free parameters. For both models, we found $T_{1,S} = 77$ ns, $T_{2,S} = 12.5$ ns, and $T_{1,V} \geq T_{2,V} \geq 5$ μs . For the shallow donor case, we found $B_1 = 0.14$ mT, $k_{\parallel} = 18$ μs^{-1} , and $k_D \leq 10$ μs^{-1} . For the shallow acceptor case, we found that the donor values multiplied by the ratio of the spin degeneracies, i.e., $(2S_V^{[0]} + 1)/(2S_V^{[-]} + 1) = 3/4$, produced a good fit as this conserves the total parameter value through all spin channels. A table of all simulation parameters corresponding to each plot can be found in the Supplementary Information.

Figure 3 shows EDMR simulations of V1a silicon vacancy-related spin pairs at low microwave power, contrasted at room temperature and low temperature, exhibiting predicted resolved hyperfine splitting due to ^{13}C , ^{29}Si , and ^{14}N nuclei. The “Central Line” is the overlapping spectra of the P_{000} deep level configuration (no ^{13}C or ^{29}Si near the silicon vacancy) and the middle peak of the hyperfine-split shallow level spectrum. Donor model simulations for different values of $A_{\parallel,29Si}^{[0]}$ and for varying Gaussian distributions of k_{\parallel} are shown in Figures 1 and 2 in the Supplementary Information. Our theory predicts that, while resolving the hyperfine structure of the silicon vacancy may be possible at room temperature, the shallow level hyperfine structure may only be resolvable at lower temperatures due to the short coherence times.

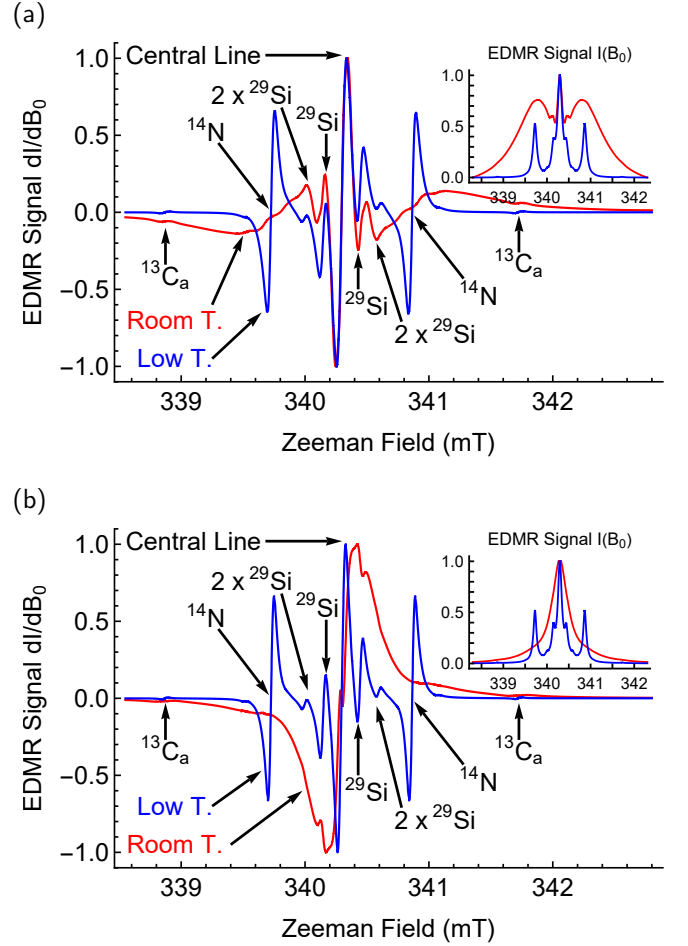


FIG. 3. The predicted EDMR spectrum (dI/dB_0) of V1a silicon vacancy-related spin pairs in 4H-SiC normalized to the peak height at low microwave power, contrasting room temperature (red) and low temperature (blue) spectra. Features arising from hyperfine splitting are identified with arrows. (a) Shallow donor model, $B_1 = 0.05$ mT. Low (Room) temperature parameters: $T_{1,S} = 1$ μs (77 ns), $T_{2,S} = 1$ μs (12.5 ns), $k_{\parallel} = 1$ μs^{-1} (18 μs^{-1}). (b) Shallow acceptor model, $B_1 = 0.0375$ mT. Low (Room) temperature parameters: $T_{1,S} = 1$ μs (77 ns), $T_{2,S} = 1$ μs (12.5 ns), $k_{\parallel} = 1$ μs^{-1} (13.5 μs^{-1}). (Insets): Corresponding simulation of the integrated EDMR spectrum $I(B_0)$ versus magnetic field.

Figure 4 illustrates the EDMR spectrum of V2a silicon vacancy-related spin pairs at low microwave power, contrasted at room temperature and low temperature, exhibiting the same hyperfine structure of both spin centers as in Figure 3. We take similar simulation parameters as in Figure 3 but now with $\mathcal{D}^{[0]} = 70$ MHz and $\mathcal{D}^{[-]} = 35$ MHz, which gives the same zero field splitting energy for both charge states. Donor model simulations for different values of $\mathcal{D}^{[0]}$ are shown in Figure 3 in the Supplementary Information. Notably, the simulations in Figure 4 predict that two-photon, double quantum transitions ($V_{2a}^{(2p)}$) between $|\pm 3/2\rangle \leftrightarrow |\mp 1/2\rangle$ states of the negatively-charged silicon vacancy may be read-out electrically in either model. While optical read-out of these double-quantum transitions has been demonstrated^{7,33}, elec-

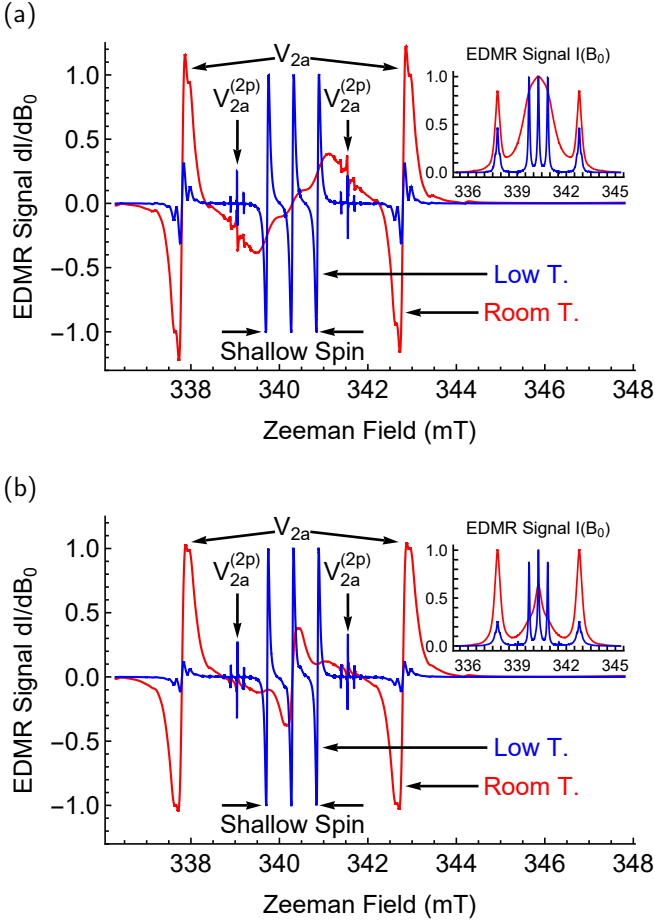


FIG. 4. The predicted EDMR spectrum (dI/dB_0) of V2a silicon vacancy-related spin pairs in 4H-SiC normalized to the peak height at low microwave power, contrasting room temperature (red) and low temperature (blue) spectra. Features arising from each spin in the pair are identified with arrows. Similar simulation parameters were used here as in Figure 3, except for $D^{[q]} \neq 0$. (a) Shallow donor model. (b) Shallow acceptor model. (Insets): Corresponding simulation of the integrated EDMR spectrum $I(B_0)$ versus magnetic field.

trical read-out would provide an avenue to enhance magnetic field sensitivity^{34,35} in all-electric magnetometers^{8,36}.

We now present the details of our theory for simulating EDMR measurements of silicon vacancy-related spin pairs. In Figs. 2-4 we modeled the EDMR dynamics with a Lindblad master equation^{37,38} of the form:

$$\begin{aligned} \partial_t \hat{\rho}(t) = & -\frac{i}{\hbar} \left[\hat{\mathcal{H}}(t), \hat{\rho}(t) \right] + \sum_i \hat{\mathcal{L}}_{hop.} [\hat{L}_i] + \sum_i \hat{\mathcal{L}}_{dec.} [\hat{L}_i] \\ \hat{\mathcal{L}} [\hat{L}_i] \equiv & k_i \left(\hat{L}_i \hat{\rho}(t) \hat{L}_i^\dagger - \frac{1}{2} \left\{ \hat{L}_i^\dagger \hat{L}_i, \hat{\rho}(t) \right\} \right) \end{aligned} \quad (3)$$

where $\hat{\mathcal{H}}(t)$ is block diagonal in $\hat{\mathcal{H}}_{1 \otimes 0}$, $\hat{\mathcal{H}}_{1 \otimes 1/2}$, and $\hat{\mathcal{H}}_{3/2 \otimes 0}$ (donor model) or $\hat{\mathcal{H}}_{3/2 \otimes 0}$, $\hat{\mathcal{H}}_{3/2 \otimes 1/2}$, and $\hat{\mathcal{H}}_{1 \otimes 0}$ (acceptor model); $\hat{\mathcal{L}}_{hop.}$ are the Lindblad superoperators for hopping processes in Figures 1 and S1; $\hat{\mathcal{L}}_{dec.}$ are the Lindblad superoperators for onsite decoherence; and \hat{L}_i are the jump operators with respective rates k_i . Calculations are done in the rotating

frame after performing the rotating wave approximation for computational ease. Additional calculation details are provided in the Supplementary Information.

The steady-state recombination current is determined by the density matrix populations of the manifold involved in recombination, i.e. the configuration corresponding to $\hat{\mathcal{H}}_{3/2 \otimes 0}$ (donor model) or $\hat{\mathcal{H}}_{1 \otimes 0}$ (acceptor model). This is achieved with the following current operator and steady-state current:

$$\hat{I} \equiv e \sum_j k_{R,j} \hat{L}_{R,j}^\dagger \hat{L}_{R,j} \quad I(B_0) \equiv Tr [\hat{I} \hat{\rho}_{ss}] \quad (4)$$

where e is the elementary charge, $k_{R,j}$ and $\hat{L}_{R,j}$ are the recombination rates and jump operators, and $\hat{\rho}_{ss}$ is the steady-state solution of Eq. (3). The current operator in Eq. (4) has the effect of tracing over the total population in the $\rho_{3/2 \otimes 0}$ manifold (donor model) or $\rho_{1 \otimes 0}$ (acceptor model).

This work presents a vital step toward optimizing SiC power electronics and EDMR-based magnetometer technology with a fully-quantitative theory of the recombination mechanism of silicon vacancy-related spin pairs in EDMR measurements using steady-state Lindblad equations. By fitting our model to experimental data attributed to V1a silicon vacancies, we constrained spin coherence times and electrical transport rates. Furthermore, we identified the shallow level spin center as a nitrogen-related complex and extracted its room-temperature coherence times. We also predicted how EDMR measurements of V1a and V2a silicon vacancy-related spin pairs are expected to respond to reduced temperatures. We conclude that while the silicon vacancy hyperfine structure may be resolvable at room temperature and at low microwave power, the shallow level hyperfine splitting may only emerge at lower temperatures due to its short coherence times. Finally, through EDMR simulations of V2a silicon vacancy-related spin pairs, we predict the emergence of two-photon double-quantum transitions which would offer an avenue towards all-electric enhanced magnetic field sensing.

This work also advances previous theories^{39,40} of EDMR by generalizing the spin-selective jump operators for $S > 1/2$, widening the applicability of these theories to include spin pairs in most electrically-active charge states. Finally, this work shows how the effects of finite coherence times can be treated with the Lindblad formalism for $S = 1/2, 1,$ and $3/2$, which are vital to the simulation of other spin-dependent readout techniques such as optically detected magnetic resonance^{41,42}, near-zero field magnetoresistance^{39,40,43}, and spin-polarized transport⁴⁴ measurements under realistic noise conditions.

ACKNOWLEDGMENTS

This material is based upon work supported by AFOSR FA9550-22-1-0308 and the NASA SC Space Grant Consortium. A portion of this research was carried out at the Jet Propulsion Laboratory, California Institute of Technology, under contract with the National Aeronautics and Space Administration, (contract 80NM0018D0004).

DATA AVAILABILITY STATEMENT

The data that support the findings of this study are included in this published article and its supplementary information files.

REFERENCES

- ¹L. F. S. Alves, R. C. M. Gomes, P. Lefranc, R. De A. Pegado, P.-O. Jeannin, B. Luciano, and F. V. Rocha, "SiC power devices in power electronics: An overview," in *2017 Brazilian Power Electronics Conference (COBEP)* (2017) pp. 1–8.
- ²C. J. Cochrane, P. M. Lenahan, and A. J. Lelis, "Deep level defects which limit current gain in 4H SiC bipolar junction transistors," *Applied Physics Letters* **90**, 123501 (2007).
- ³C. J. Cochrane, P. M. Lenahan, and A. J. Lelis, "An electrically detected magnetic resonance study of performance limiting defects in SiC metal oxide semiconductor field effect transistors," *Journal of Applied Physics* **109**, 014506 (2011).
- ⁴S. J. Pearton, A. Aitkaliyeva, M. Xian, F. Ren, A. Khachatryan, A. Ildonfonso, Z. Islam, M. A. Jafar Rasel, A. Haque, A. Y. Polyakov, and J. Kim, "Review—Radiation Damage in Wide and Ultra-Wide Bandgap Semiconductors," *ECS Journal of Solid State Science and Technology* **10**, 55008 (2021).
- ⁵M. Widmann, S.-Y. Lee, T. Rendler, N. T. Son, H. Fedder, S. Paik, L.-P. Yang, N. Zhao, S. Yang, I. Booker, A. Denisenko, M. Jamali, S. A. Momenzadeh, I. Gerhardt, T. Ohshima, A. Gali, E. Janzén, and J. Wrachtrup, "Coherent control of single spins in silicon carbide at room temperature," *Nature Materials* **14**, 164–168 (2015).
- ⁶K. Tahara, S.-i. Tamura, H. Toyama, J. J. Nakane, K. Kutsuki, Y. Yamazaki, and T. Ohshima, "Quantum sensing with duplex qubits of silicon vacancy centers in SiC at room temperature," *npj Quantum Information* **11**, 58 (2025).
- ⁷H. Kraus, V. Soltamov, D. Riedel, S. Váth, F. Fuchs, A. Sperlich, P. Baranov, V. Dyakonov, and G. Astakhov, "Room-temperature quantum microwave emitters based on spin defects in silicon carbide," *Nature Physics* **10**, 157–162 (2014).
- ⁸C. J. Cochrane, J. Blacksborg, M. A. Anders, and P. M. Lenahan, "Vectorized magnetometer for space applications using electrical readout of atomic scale defects in silicon carbide," *Scientific Reports* **6**, 37077 (2016).
- ⁹A. Gottscholl, H. Kraus, T. Aichinger, and C. J. Cochrane, "Enhancing the electrical readout of the spin-dependent recombination current in SiC JFETs for EDMR based magnetometry using a tandem (de-)modulation technique," *Scientific Reports* **14**, 14283 (2024).
- ¹⁰C. T.-K. Lew, V. K. Sewani, N. Iwamoto, T. Ohshima, J. C. McCallum, and B. C. Johnson, "Enhanced magnetometry with an electrically detected spin defect ensemble in silicon carbide," *Applied Physics Letters* **122**, 234001 (2023).
- ¹¹C. T.-K. Lew, V. K. Sewani, N. Iwamoto, T. Ohshima, J. C. McCallum, and B. C. Johnson, "All-Electrical Readout of Coherently Controlled Spins in Silicon Carbide," *Phys. Rev. Lett.* **132**, 146902 (2024).
- ¹²H. Kraus, V. Soltamov, F. Fuchs, D. Simin, A. Sperlich, P. Baranov, G. Astakhov, and V. Dyakonov, "Magnetic field and temperature sensing with atomic-scale spin defects in silicon carbide," *Scientific Reports* **4**, 5303 (2014).
- ¹³I. Lekavicius, S. Carter, D. Pennachio, S. White, J. Hajzus, A. Purdy, D. Gaskill, A. Yeats, and R. Myers-Ward, "Magnetometry Based on Silicon-Vacancy Centers in Isotopically Purified 4H-SiC," *Phys. Rev. Appl.* **19**, 044086 (2023).
- ¹⁴Y. Yamazaki, Y. Masuyama, K. Kojima, and T. Ohshima, "Highly Sensitive Temperature Sensing Using the Silicon Vacancy in Silicon Carbide by Simultaneously Resonated Optically Detected Magnetic Resonance," *Phys. Rev. Appl.* **20**, L031001 (2023).
- ¹⁵E. Sörman, N. T. Son, W. M. Chen, O. Kordina, C. Hallin, and E. Janzén, "Silicon vacancy related defect in 4H and 6H SiC," *Phys. Rev. B* **61**, 2613–2620 (2000).
- ¹⁶N. Mizuochi, S. Yamasaki, H. Takizawa, N. Morishita, T. Ohshima, H. Itoh, and J. Isoya, "Continuous-wave and pulsed EPR study of the negatively charged silicon vacancy with $S = \frac{3}{2}$ and C_{3v} symmetry in n -type 4H-SiC," *Phys. Rev. B* **66**, 235202 (2002).
- ¹⁷C. J. Cochrane, P. M. Lenahan, and A. J. Lelis, "An electrically detected magnetic resonance study of performance limiting defects in SiC metal oxide semiconductor field effect transistors," *Journal of Applied Physics* **109**, 014506 (2011).
- ¹⁸M. Suckert, F. Hoehne, L. Dreher, M. Kuenzl, H. Huebl, M. Stutzmann, and M. S. Brandt, "Electrically detected double electron-electron resonance: exchange interaction of 31P donors and Pb0 defects at the Si/SiO2 interface," *Molecular Physics* **111**, 2690–2695 (2013).
- ¹⁹F. Hoehne, L. Dreher, M. Suckert, D. P. Franke, M. Stutzmann, and M. S. Brandt, "Time constants of spin-dependent recombination processes," *Phys. Rev. B* **88**, 155301 (2013).
- ²⁰C. J. Cochrane, P. M. Lenahan, and A. J. Lelis, "Identification of a silicon vacancy as an important defect in 4H SiC metal oxide semiconducting field effect transistor using spin dependent recombination," *Applied Physics Letters* **100**, 023509 (2012).
- ²¹N. Mizuochi, S. Yamasaki, H. Takizawa, N. Morishita, T. Ohshima, H. Itoh, and J. Isoya, "EPR studies of the isolated negatively charged silicon vacancies in n -type 4H- and 6H-SiC: Identification of C_{3v} symmetry and silicon sites," *Phys. Rev. B* **68**, 165206 (2003).
- ²²S. Greulich-Weber, "EPR and ENDOR Investigations of Shallow Impurities in SiC Polytypes," *Physica Status Solidi (a)* **162**, 95–151 (1997).
- ²³N. T. Son, J. Isoya, T. Umeda, I. G. Ivanov, A. Henry, T. Ohshima, and E. Janzén, "EPR and ENDOR Studies of Shallow Donors in SiC," *Applied Magnetic Resonance* **39**, 49–85 (2010).
- ²⁴A. v. Duijn-Arnold, R. Zondervan, J. Schmidt, P. G. Baranov, and E. N. Mokhov, "Electronic structure of the N donor center in 4H-SiC and 6H-SiC," *Phys. Rev. B* **64**, 085206 (2001).
- ²⁵N. T. Son, E. Janzén, J. Isoya, and S. Yamasaki, "Hyperfine interaction of the nitrogen donor in 4H-SiC," *Phys. Rev. B* **70**, 193207 (2004).
- ²⁶H. H. Woodbury and G. W. Ludwig, "Electron Spin Resonance Studies in SiC," *Phys. Rev.* **124**, 1083–1089 (1961).
- ²⁷R. J. Waskiewicz, B. R. Manning, D. J. McCrory, and P. M. Lenahan, "Electrically detected electron nuclear double resonance in 4H-SiC bipolar junction transistors," *Journal of Applied Physics* **126**, 125709 (2019).
- ²⁸E. Higa, M. Sometani, H. Hirai, H. Yano, S. Harada, and T. Umeda, "Electrically detected magnetic resonance study on interface defects at nitrided Si-face, a-face, and m-face 4H-SiC/SiO2 interfaces," *Applied Physics Letters* **116**, 171602 (2020).
- ²⁹C. J. Cochrane, P. M. Lenahan, and A. J. Lelis, "The effect of nitric oxide anneals on silicon vacancies at and very near the interface of 4H SiC metal oxide semiconducting field effect transistors using electrically detected magnetic resonance," *Applied Physics Letters* **102**, 193507 (2013).
- ³⁰M. A. Anders, P. M. Lenahan, A. H. Edwards, P. A. Schultz, and R. M. Van Ginhoven, "Effects of nitrogen on the interface density of states distribution in 4H-SiC metal oxide semiconductor field effect transistors: Super-hyperfine interactions and near interface silicon vacancy energy levels," *Journal of Applied Physics* **124**, 184501 (2018).
- ³¹R. Kosugi, T. Umeda, and Y. Sakuma, "Fixed nitrogen atoms in the SiO2/SiC interface region and their direct relationship to interface trap density," *Applied Physics Letters* **99**, 182111 (2011).
- ³²J. Rozen, S. Dhar, M. E. Zvanut, J. R. Williams, and L. C. Feldman, "Density of interface states, electron traps, and hole traps as a function of the nitrogen density in SiO2 on SiC," *Journal of Applied Physics* **105**, 124506 (2009).
- ³³H. Singh, M. A. Hollberg, A. N. Anisimov, P. G. Baranov, and D. Suter, "Multi-photon multi-quantum transitions in the spin- $\frac{3}{2}$ silicon-vacancy centers of sic," *Phys. Rev. Res.* **4**, 023022 (2022).
- ³⁴A. Dréau, M. Lesik, L. Rondin, P. Spinicelli, O. Arcizet, J.-F. Roch, and V. Jacques, "Avoiding power broadening in optically detected magnetic resonance of single NV defects for enhanced dc magnetic field sensitivity," *Phys. Rev. B* **84**, 195204 (2011).
- ³⁵J. F. Barry, J. M. Schloss, E. Bauch, M. J. Turner, C. A. Hart, L. M. Pham, and R. L. Walsworth, "Sensitivity optimization for NV-diamond magnetometry," *Rev. Mod. Phys.* **92**, 015004 (2020).
- ³⁶W. Baker, K. Ambal, D. Waters, R. Baarda, H. Morishita, K. van Schooten, D. McCamey, J. Lupton, and C. Boehme, "Robust absolute magnetometry

- with organic thin-film devices,” *Nature Communications* **3**, 898 (2012).
- ³⁷V. Gorini, A. Kossakowski, and E. C. G. Sudarshan, “Completely positive dynamical semigroups of N-level systems,” *Journal of Mathematical Physics* **17**, 821–825 (1976).
- ³⁸G. Lindblad, “On the generators of quantum dynamical semigroups,” *Communications in Mathematical Physics* **48**, 119–130 (1976).
- ³⁹N. J. Harmon, J. P. Ashton, P. M. Lenahan, and M. E. Flatté, “Spin-dependent capture mechanism for magnetic field effects on interface recombination current in semiconductor devices,” *Applied Physics Letters* **123**, 251603 (2023).
- ⁴⁰N. J. Harmon, S. R. Mcmillan, J. P. Ashton, P. M. Lenahan, and M. E. Flatté, “Modeling of Near Zero-Field Magnetoresistance and Electrically Detected Magnetic Resonance in Irradiated Si/SiO₂ MOSFETs,” *IEEE Transactions on Nuclear Science* **67**, 1669–1673 (2020).
- ⁴¹R. N. Patel, R. E. K. Fishman, T.-Y. Huang, J. A. Gusdorff, D. A. Fehr, D. A. Hopper, S. A. Breitweiser, B. Porat, M. E. Flatté, and L. C. Bassett, “Room Temperature Dynamics of an Optically Addressable Single Spin in Hexagonal Boron Nitride,” *Nano Letters* **24**, 7623–7628 (2024).
- ⁴²M. A. Sadi, L. Basso, D. A. Fehr, X. Gao, S. Vaidya, E. G. Riendeau, G. Joshi, T. Li, M. E. Flatté, A. M. Mounce, and Y. P. Chen, “Spin-State-Selective Excitation in Spin Defects of Hexagonal Boron Nitride,” *Nano Letters* **25**, 12067–12074 (2025).
- ⁴³M. J. Elko, D. T. Hassenmayer, A. A. Higgins, P. M. Lenahan, M. E. Flatté, D. Fehr, M. D. Craven, and T. D. Larsen, “Near zero-field magnetoresistance and defects in gallium nitride pn junctions,” *Journal of Vacuum Science & Technology B* **42**, 052205 (2024).
- ⁴⁴S. R. McMillan, N. J. Harmon, and M. E. Flatté, “Image of Dynamic Local Exchange Interactions in the dc Magnetoresistance of Spin-Polarized Current through a Dopant,” *Phys. Rev. Lett.* **125**, 257203 (2020).